

# Universal properties of primary and secondary cosmic ray energy spectra

Marco Smolla<sup>1,2</sup>, Benjamin Schäfer<sup>3</sup>, Harald Lesch<sup>2</sup> and Christian Beck<sup>3</sup>

<sup>1</sup> Max-Planck-Institut für extraterrestrische Physik, Giessenbachstrasse, 85741 Garching, Germany

<sup>2</sup> Ludwig-Maximilians-Universität München, Universitäts-Sternwarte München, Scheinerstrasse 1, 81679 München, Germany

<sup>3</sup> School of Mathematical Sciences, Queen Mary University of London, London E1 4NS, United Kingdom

E-mail: [smolla@mpe.mpg.de](mailto:smolla@mpe.mpg.de)

E-mail: [b.schaefer@qmul.ac.uk](mailto:b.schaefer@qmul.ac.uk)

E-mail: [c.beck@qmul.ac.uk](mailto:c.beck@qmul.ac.uk)

## Abstract.

Atomic nuclei appearing in cosmic rays are typically classified as primary or secondary. However, a better understanding of their origin and propagation properties is still necessary. We analyse the flux of primary (He, C, O) and secondary nuclei (Li, Be, B) detected with rigidity (momentum/charge) between 2 GV and 3 TV by the Alpha Magnetic Spectrometer (AMS) on the International Space Station. We show that  $q$ -exponential distribution functions, as motivated by generalized versions of statistical mechanics with temperature fluctuations, provide excellent fits for the measured flux of all nuclei considered. Primary and secondary fluxes reveal a universal dependence on kinetic energy per nucleon for which the underlying energy distribution functions are solely distinguished by their effective degrees of freedom. All given spectra are characterized by a universal mean temperature parameter  $\sim 200$  MeV which agrees with the Hagedorn temperature. Our analysis suggests that QCD scattering processes together with nonequilibrium temperature fluctuations imprint universally onto the measured cosmic ray spectra, and produce a similar shape of energy spectra as high energy collider experiments on the Earth.

*Keywords:* Cosmic Rays, High-Energy Physics, Generalized Statistical Mechanics

Submitted to: *New J. Phys.*

## 1. Introduction

A fundamental challenge of current cosmic ray (CR) research is to understand the origin of highly energetic CRs, their abundance in terms of different particle types, and to identify the processes at work for acceleration and propagation. Collectively these processes determine the energy dependent flux of CRs, that is their energy spectra. Because charged particles gyrate around the magnetic field lines of the interstellar medium (ISM), the directional information about the source is ultimately lost, leading to a roughly isotropic distribution observed here at Earth. The atomic nuclei among the CRs are classified as primary CRs, usually thought to be expelled by supernovae explosions and accelerated in shock fronts of supernova remnants, and secondary CRs, which result from particle collisions in the ISM. Here, we consider the flux of six different nuclei, namely the primaries He, C, O and the secondaries Li, Be, B as observed with the Alpha Magnetic Spectrometer (AMS) on the International Space Station [1, 2].

It is commonly accepted that the major fraction of He, C, O can be classified as primary CRs whereas Li, Be, B are secondary CRs because their relative abundance exceeds the chemical composition of the ISM by a few orders of magnitude [3]. Some progress has been made in explaining CR acceleration (e.g. at supernova remnant shocks) [4] and propagation (e.g. diffusion confinement) [5] which allows to better investigate the specific processes responsible for the observed distributions. Nevertheless, considering the multitude of physical processes involved, our understanding remains incomplete and theoretical models accounting for the given nuclei spectra contain many unknown parameters and are currently under debate [6].

As measured cosmic ray energy spectra decay in good approximation with a power law over many orders of magnitudes, it is reasonable to apply a generalized statistical mechanics formalism (GSM) [7] which generates power laws rather than exponential distributions as the relevant effective canonical distributions. Canonical Boltzmann-Gibbs (BG) statistics is only valid in an equilibrium context for systems with short-range interactions, but it can be generalized to a nonequilibrium context by introducing an entropic index  $q$ , where  $q > 1$  accounts for heavy-tailed statistics and  $q = 1$  recovers BG statistics [8, 9, 10]. The occurrence of the index  $q$  can be naturally understood due to the fact that there are spatio-temporal temperature fluctuations in a general nonequilibrium situation, as addressed by the general concept of superstatistics, a by now standard statistical physics method [11]. Since the flux distribution as a function of energy in CRs evidently does not decay exponentially, it is reasonable not to use BG statistics but rather GSM, which has been successfully applied to cosmic rays before in [12, 13, 14] and also applied to particle collisions in LHC experiments [15, 16, 17]. Other applications of this superstatistical nonequilibrium approach are Lagrangian [18] and defect turbulence [19], fluctuations in wind velocity and its persistence statistics [20, 21], fluctuations in the power grid frequency [22, 23] and air pollution statistics [24].

Here, we apply GSM and superstatistical methods to the observed CR flux of

atomic nuclei to infer the physical parameters of the underlying energy distributions, which turn out to be nearly identical for all primaries and secondaries, respectively. The universal properties of the two CR types can be distinguished by a single parameter, the entropic index  $q$ , which we relate to the effective degrees of freedom of temperature fluctuations that are relevant in a GSM description. The average temperature parameter that fits all nuclei spectra turns out to be universal as well and is given by about 200 MeV, coinciding with the Hagedorn temperature. This suggests that QCD scattering processes play a dominant role in shaping the spectrum of observed cosmic rays. The spectra are indeed similar to observed momentum spectra in high energy proton-proton-collider experiments on the Earth, which are known to generate  $q$ -exponential power laws [17, 15].

The paper is organized as follows: In section 2 we demonstrate that cosmic ray nuclei spectra, as measured by AMS, are well described by  $q$ -exponential distribution functions. We show that the spectra exhibit data collapse if they are related to the kinetic energy per nucleon. In section 3 we interpret the observed spectra in terms of temperature fluctuations occurring during the production process of the cosmic rays, based on  $\chi^2$  superstatistics. We relate the power law spectral index to the relevant degrees of freedom contributing to the temperature fluctuations. Finally, a possible physical explanation of the universal properties of the observed spectra is given in section 4.

## 2. Results

We investigate the cosmic ray flux, given as differential intensity with respect to kinetic energy per nucleon, defined as  $E = (E_{total} - m)/A$ , with total energy  $E_{total} = \sqrt{p^2 + m^2}$ , momentum  $p = |\vec{p}|$ , rest mass  $m = Au$ , mass number  $A$ , atomic mass unit  $u = 0.931$  GeV and  $[m] = [p] = [\text{GeV}]$  in  $c = 1$  convention.

In order to infer physical parameters from the energy distribution fit to the observed cosmic ray flux, we employ an established GSM model [13], modified slightly by replacing the total energy by the kinetic energy per nucleon  $E$ . [This choice of variable is common practice in CR literature because the kinetic energy per nucleon and the charge to mass ratio of a given particle provides the essential properties that decide how the particle's trajectory will be modified by the presence of magnetic field lines.](#) In the Appendix we rigorously derive the distribution function

$$P_E(E) = C\rho(E)e_q^{-bE}, \quad (1)$$

which corresponds to the following differential intensity of flux

$$J_E(E) = v(E)P_E, \quad (2)$$

where  $C$ ,  $q > 1$  and  $T = b^{-1} > 0$  are free parameters and the  $q$ -exponential is defined as  $e_q^x \equiv (1 + (1 - q)x)^{\frac{1}{1-q}}$  which implies  $e_{q \rightarrow 1}^x = e^x$ .  $\rho(E)$  is a phase space factor which describes the density of states, i.e. how many energy states can be taken on in a given

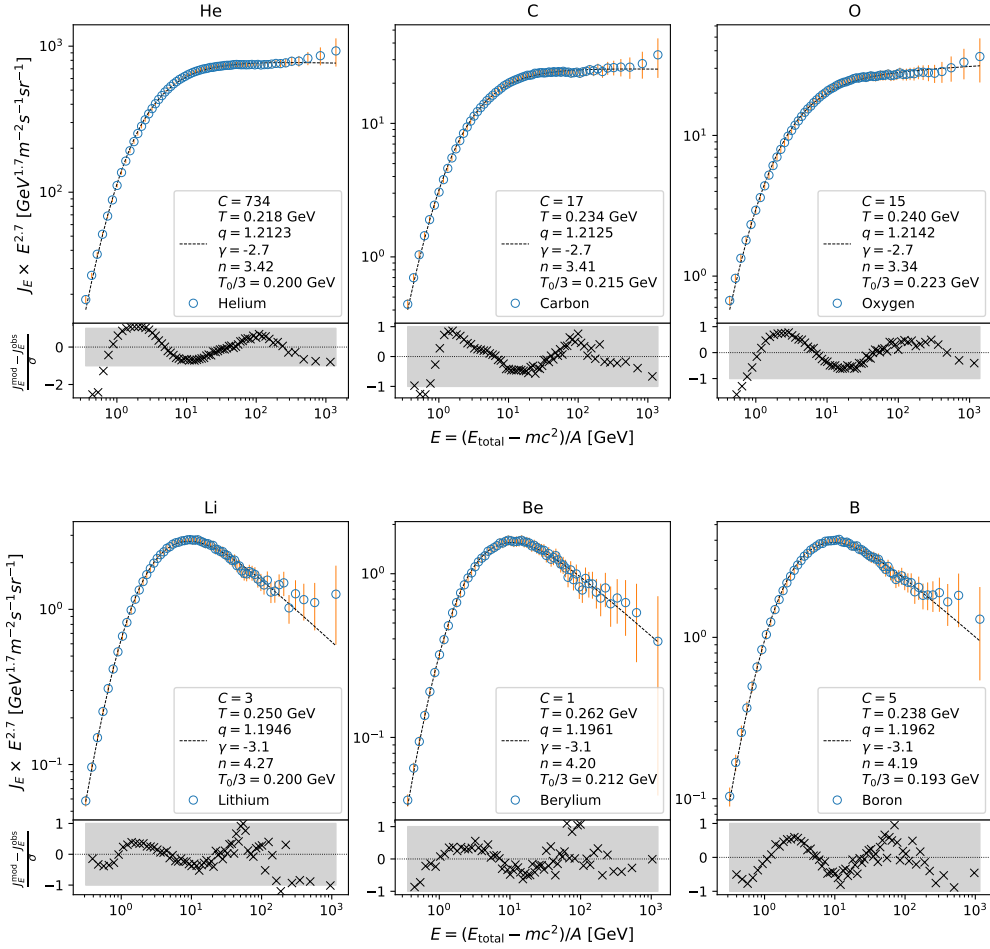


**Figure 1.** The particle flux of each CR species was fitted with (3) using three parameters  $C, T, q$ . The vertical axis in this log-log plot was multiplied with  $E^{2.7}$  for better visibility. The fit's accuracy can be quantified by the deviation from modelled  $J^{mod}$  to observed flux  $J^{obs}$  weighted by the respective measurement error  $\sigma$ . Evidently, almost all data points fall within the uncertainty range of  $\pm\sigma$  illustrated as grey shaded area. The mean temperature  $T_0$  is defined by (9). The amplitude  $C$  has dimensions  $[C] = [\text{m}^{-2} \text{sr}^{-1} \text{s}^{-1} \text{GeV}^{-3}]$ .

range. For our fits we used  $\rho(E) = p^2 \frac{dp}{dE} = (E + u) \sqrt{E(E + 2u)}$  which leads to the flux derived from our superstatistical model

$$J_E^{mod}(E) = CE(E + 2u)e_q(-bE), \quad (3)$$

which we compare to the observed flux  $J_E^{obs}$ .

The entropic index  $q$  determines the high-energy (i.e. the tail) behavior of the distribution since the  $q$ -exponential asymptotically approaches a power law

$$\lim_{E \rightarrow \infty} e_q^{-bE} \propto E^\gamma, \quad (4)$$

with spectral index  $\gamma = 2 - 1/(q - 1)$  for  $q > 1$ . The parameter  $T = b^{-1}$  represents a temperature in energy units that constrains the low-energy regime of maximum flux.

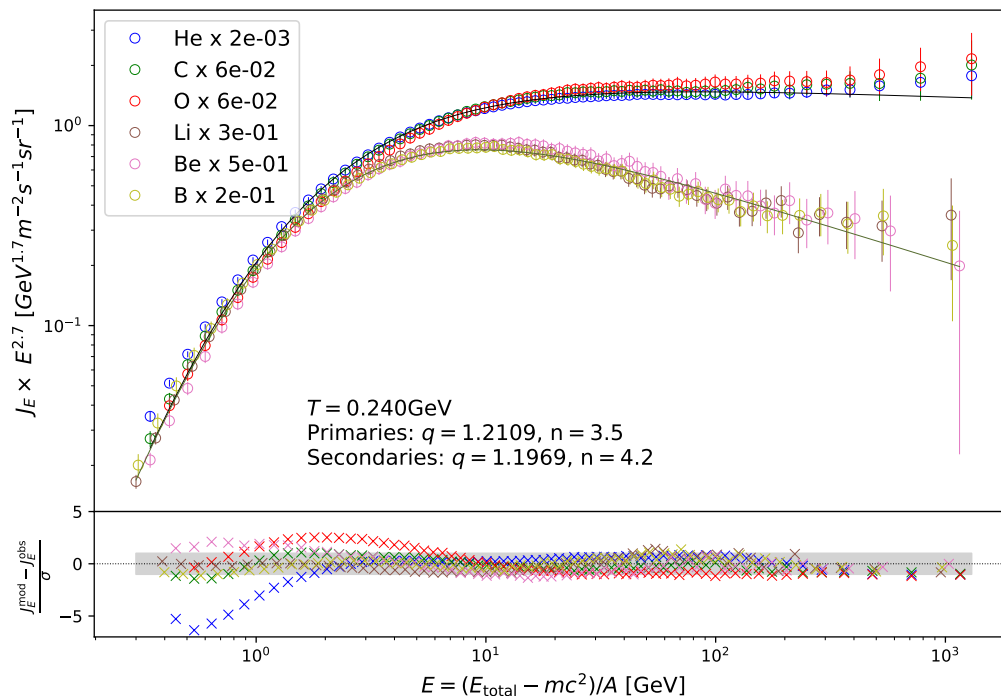


**Figure 2.** Each particle flux was rescaled with a suitable factor such that the data points (roughly) collapse to a single line at the low energy end and the universal properties of primary and secondary cosmic ray nuclei spectra become visible. For larger energies the spectrum splits into primaries and secondaries which can be distinguished by a single parameter, the entropic index  $q$  which can be interpreted by the underlying effective degrees of freedom.

Since our analysis focuses on the spectral *shape* of the energy distribution we collect all global factors, which do not depend explicitly on the energy, in the amplitude  $C$ , which is merely a gauge for the absolute magnitude of the flux.

Fig. 1 illustrates that most data points are fitted by our model within a single standard deviation for all six nuclei. We determined the best fit by applying  $\chi^2$  minimisation with  $(J_E^{\text{mod}} - J_E^{\text{obs}})/\sigma$ , meaning deviation of model from data weighted by the respective measurement uncertainty, where the standard deviation  $\sigma$  is the sum of measurement errors for a specific energy bin. For most of the data the error is of the order of a few percent whereas the uncertainty tends to increase with energy up to the largest uncertainty of 89 percent associated with the Beryllium flux measured in the highest energy bin.

Fig. 2 reveals the universal properties of the primary (He, C, O) and secondary (Li, Be, B) cosmic ray fluxes when rescaling each nuclei flux with a suitable global factor such that all data points collapse to a single line in the low energy range. Fixing the

global amplitude parameter to  $C = 1$  and  $T = 0.240$  GeV, which is the average value for the temperatures inferred from the individual best fits in Fig. 1, allows us to do a best fit with  $q$  as the only free parameter for the collapsed data of primaries and secondaries. This yields  $q_{\text{prim}} = 1.2109$  ( $n = 3.5$ ) and  $q_{\text{sec}} = 1.1969$  ( $n = 4.2$ ), where  $n$  can be interpreted as degrees of freedom of temperature fluctuations as outlined below.

### 3. Interpretation in terms of temperature fluctuations

We consider the observed cosmic ray spectra to be the result of many different high energy scattering processes, each having a different local temperature  $\beta^{-1}$  in the local scattering volume. This idea was previously worked out in detail for collider experiments using LHC data, e.g. in [15]. There are strong fluctuations of temperature in each scattering event, which can be described by superstatistics [11], a standard method in the theory of complex systems. For cosmic rays, we need to generate asymptotic power laws and this can be achieved by so-called  $\chi^2$  superstatistics. As is generally known (see, e.g. [13]) the probability density function for a fluctuating  $\beta$  of the form

$$\beta = \sum_{i=1}^n X_i^2 \quad (5)$$

with independent and identically distributed Gaussian random variables  $X_i$  is a  $\chi^2$  distribution given by

$$g(\beta) = \frac{1}{\Gamma(n/2)} \left( \frac{n}{2\beta_0} \right)^{\frac{n}{2}} \beta^{\frac{n}{2}-1} \exp\left(-\frac{n\beta}{2\beta_0}\right). \quad (6)$$

It is well-known in the formalism of superstatistics that superimposing various subsystems with different temperature weighted with  $g(\beta)$  leads to  $q$ -exponential statistics. For each scattering event we apply ordinary statistical mechanics locally, i.e. the conditional probability density of a kinetic energy state  $E$  in a given scattering event for a given temperature is

$$p_E(E|\beta) = \frac{1}{Z(\beta)} \rho(E) e^{-\beta E}. \quad (7)$$

In order to normalize our conditional distribution function we need to integrate over all possible energy states, obtaining the normalization constant  $Z(\beta) = \int_0^\infty \rho(E) e^{-\beta E} dE$ . The marginal distribution  $P_E(E)$  (the unconditioned distribution of energies) can be computed by integrating the conditional distribution  $p_E(E|\beta)$  over all inverse temperatures  $\beta$  weighted with  $g(\beta)$ . In the relativistic limit (neglecting mass terms) this yields

$$P_E(E) = \int_0^\infty g(\beta) p_E(E|\beta) d\beta \sim \rho(E) e_q^{-bE} \quad (8)$$

with  $b = \beta_0/(4 - 3q)$  and mean inverse temperature

$$\beta_0 = \int_0^\infty \beta g(\beta) d\beta =: \frac{1}{T_0}. \quad (9)$$

The effective degrees of freedom  $n$  are related to the entropic index  $q$  via

$$n = \frac{2}{q-1} - 6. \quad (10)$$

Considering the physical meaning of the random variable  $X_i$  defined in equation (5) there are different possible interpretations, see [13, 18, 25, 26] for details. The main conclusions in our given analysis are independent of the particular interpretation chosen but it is worth emphasizing that it is physically plausible to understand  $X_i$  as a measure for the fluctuating effective energy dissipation, with  $n = 3$  representing the three spatial degrees of freedom as minimum value, which is increased to  $n = 4$  when including variations in time.

In the Appendix we provide a more detailed derivation of the above results, which show that  $q$ -exponential statistics follows naturally from summing up ordinary Boltzmann distributions with  $\chi^2$ -distributed inverse temperatures.

#### 4. Physical interpretation and possible reason for universality

For the temperature parameter  $T_0 = \beta_0^{-1}$ , defined in (9), we get the value  $T_0 \sim 600$  MeV for each of the six CR species in our fits. Hence, the average effective temperature per quark is of the order  $T_0/3 \sim 200$  MeV, i.e. we recover approximately the observed value of the Hagedorn temperature which is roughly known to be in the range 140 to 200 MeV [27, 28, 29] and represents a universal critical temperature for the quark gluon plasma and for high energy QCD scattering processes. Remarkably, the fitted value of  $T_0/3$  in the fits is observed to be the same for all six nuclei, i.e. for both primary and secondary cosmic rays within [a range of about one tenth of its absolute value](#).

Let us provide some arguments on why we consider  $T_0/3$  as a relevant temperature parameter. In general, there are two alternative formulations of superstatistics, defined as type A and type B in [11], which yield the same form of distribution functions but differ in their definitions for  $T_0$  because type A uses the unnormalized whereas type B uses the normalized Boltzmann factor for deriving the generalized canonical distribution, as we present in detail for type B in the appendix. We consider type B superstatistics as physically more plausible because we understand the generalized canonical distribution as originating from a superposition of many cosmic ray ensembles associated with a normalized canonical distribution respectively. Since the Hagedorn temperature is associated with the kinetic energy of particles interacting via the strong nuclear force, we divide the average temperature  $T_0$  by the number of quarks, namely three for atomic nuclei. For a quark-gluon plasma one can either define a temperature for single quarks, or - after hadronization - for mesonic or baryonic states. At the critical Hagedorn phase transition point, where both states exist, this is mainly a question of definition [30].

The emergence of the Hagedorn temperature (at least as an order of magnitude) in our fits suggests that cosmic ray energy spectra might originate from high energy scattering processes taking place at the Hagedorn temperature  $T_H$ . Very young

neutron stars, initially formed in a supernova explosion, indeed have a temperature  $\sim 10^{12}$  K  $\sim 100$  MeV of comparable order of magnitude as the Hagedorn temperature [31]. As the Hagedorn temperature is universal, so is the average kinetic energy per quark of the cosmic rays nuclei, assuming they are produced in a Hagedorn fireball, either during the original supernova explosion, or later in collision processes of highly energetic CR particles with the ISM.

Our observation that the kinetic energy per nucleon (or per quark) yields universal behavior of the spectra is indeed pointing towards QCD processes as the dominant contribution that shapes the spectra (see also [14]): Were there mainly electromagnetic processes underlying the spectra, one would expect invariance under rescaling with  $Z$ , but we observe invariance (universality) under rescaling with  $A$ . At the LHC one observes similar  $q$ -exponentials for the measured transverse momentum spectra, as generated by QCD scattering processes, with a temperature parameter  $b^{-1}$  that is of similar order of magnitude (150 MeV) as in our fits for the cosmic rays, see table IV in [17]. That paper also shows that hard parton QCD scattering leads to power law spectral behavior.

Note that while the entire energy spectrum in figure 1 is well fitted by a  $q$ -exponential, the residuals tend to oscillate. A similar oscillatory behavior of the residuals (logarithmically depending on the energy) has been observed in the transverse momentum distribution for high energy  $pp$  collision experiments at the LHC [32, 17]. The similarity of these log-periodic oscillations for our cosmic ray data and for collider experiments on the Earth is indeed striking, and once again supports our point that both phenomena could have similar roots based on high energy scattering processes.

After having analysed the average temperature, let us now concentrate on the *fluctuations* of temperature in the individual scattering events, described by the parameter  $n$ , which determines the entropic index  $q$  and thereby the tail behavior. One readily notices that in our GSM model the marginal distributions  $P_E(E)$  decay asymptotically as

$$P_E(E) \sim E^{-1-\frac{n}{2}}. \quad (11)$$

In order to calculate the expectation of the fluctuating energy  $E$ ,

$$\langle E \rangle = \int_0^\infty EP_E(E)dE, \quad (12)$$

one notices that the integrand decays as  $EP(E) \sim E^{-n/2}$ . Thus the expectation value is only well defined if  $n > 2$ .

In the absence of further effects, like an energy dependent cross section, we could explain  $n$  exclusively by the underlying statistics and thus associate  $n$  with the number of Gaussian random variables contributing to the fluctuating  $\beta$  in equation (5). Since for cosmic ray propagation energy dependent processes affect the spectral shape the derived value for  $n$  will represent both the statistical properties and the energy dependent processes. For this reason effective non-integer values for  $n$  are possible. Because the above argument about the existence of the expectation value should apply more



generally, and thus even in the absence of additional spectral modifications, we conclude that  $n = 3$  is the minimum value for the degrees of freedom.

A similar argument applies if one looks at the existence of the mean of the temperature  $\beta^{-1}$  as formed with the probability density  $g(\beta)$

$$\langle \beta^{-1} \rangle = \int_0^\infty \beta^{-1} g(\beta) d\beta. \quad (13)$$

The above mean only exists for  $n > 2$ , since the integrand behaves as  $\beta^{\frac{n}{2}-2}$  for  $\beta \rightarrow 0$ . We are thus naturally led to the minimum value  $n = 3$  as the strongest fluctuation state of the Hagedorn fireball for which a mean energy  $\langle E \rangle$  and a mean temperature  $\langle \beta^{-1} \rangle$  is well-defined.

For secondary cosmic rays, there is an additional degree of freedom as an additional collision process at a later time is needed to produce secondary cosmic rays. Thus it is plausible that for secondary cosmic rays  $n$  is larger than the minimum value  $n = 3$ . The next higher value of  $n$ , which can be regarded as an excited state of temperature fluctuations,  $n = 4$ , corresponds to  $q = 1.2000$ . Indeed, based on our fits (see Fig. 1), secondary cosmic rays are well approximated by this  $q$  and therefore  $n = 4$ .

In the experimental data detected by AMS, it is to be expected that we will not observe the exact values of  $q = 1.2222$  and  $q = 1.2000$  since the spectra are modified by diffusion processes in the galaxy, by energy dependent escape processes from the shock front of the accelerating supernova remnant, and by radiative losses from acceleration. All these effects can alter the spectrum and lead to small changes in the optimum fitting parameters  $q$  and  $T$ . We think this is the reason why the best fits of the observed spectra correspond to  $n = 3.5$  rather than  $n = 3$ , and  $n = 4.2$  rather than  $n = 4$ , equivalent to minor negative corrections for the spectral index  $\gamma$  of the order  $\Delta\gamma \approx -0.1$ . Also, the effective temperature  $T$  may be increased by diffusion processes in the galaxy, which will broaden the distributions. However, it seems these effects are only small perturbations that slightly modify the universal parameters set by the QCD scattering processes.

While the connection of QCD and generalized statistical mechanics was emphasized in [17], the model that we implement in our paper is mainly based on a nonequilibrium statistical mechanics approach, as originally introduced in [13]. This approach is based on temperature fluctuations in each (small) interaction volume, where the scattering event takes place. These local temperature fluctuations are at the root of the observed  $q$ -exponentials and the associated temperature scale turns out to coincide approximately with the Hagedorn temperature known from QCD. Other authors [33] have emphasized the fractal and hierarchical structure of scattering events and hadronization cascades, or the complexity of long-range interactions in the hadronization process [34, 30] coming to similar conclusions.

## 5. Discussion on relevance of solar wind modulation

The AMS measurements were taken at about 400 km above Earth's surface and are thus subject to solar wind modulation which yields a suppressed flux compared to outside the

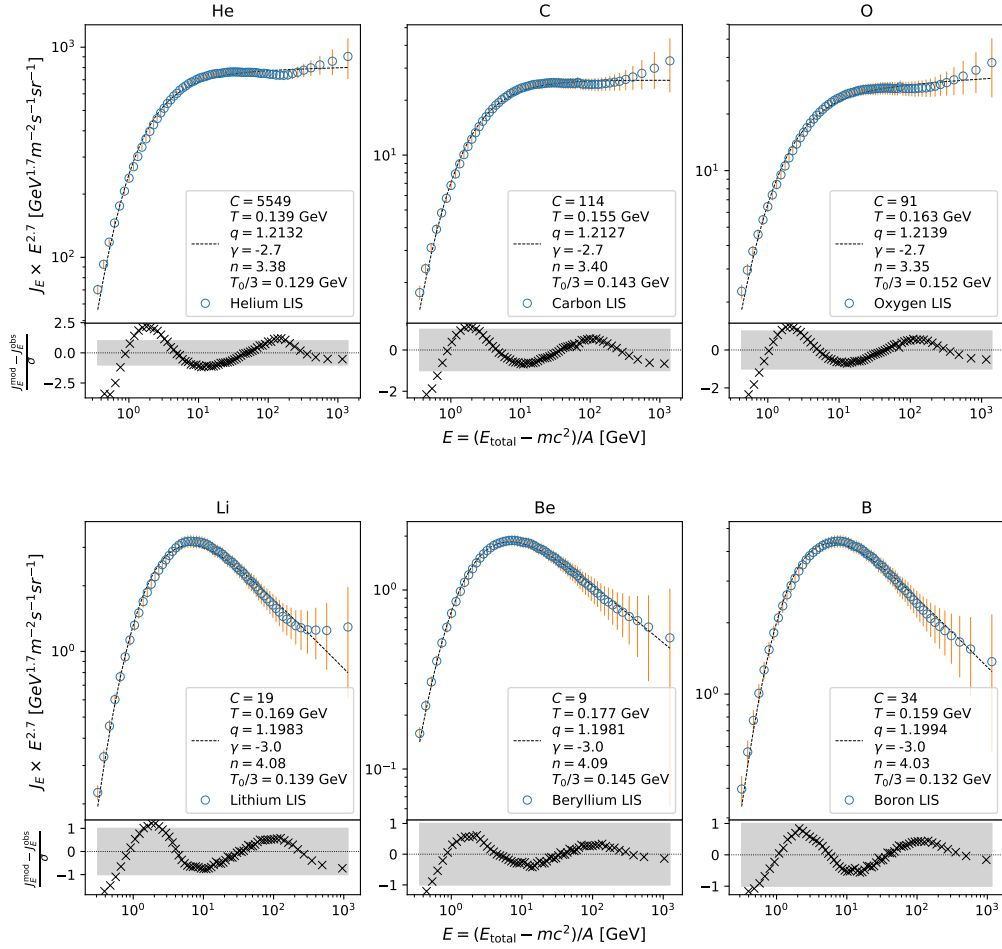


**Figure 3.** Superstatistical results are robust when correcting for heliospheric impact. Using cosmic ray propagation models HelMod and Galprop allows [35, 36, 37] to estimate flux outside the heliosphere, that is unmodulated by solar wind representing the local interstellar spectra, in short LIS. Here, we use the data published in [35, 36, 37] which we investigate for the given AMS energy bins. We apply  $J_E^{\text{mod}}(E) = CE(E + 2u)e_q(-bE)$  with  $e_q^x \equiv (1 + (1 - q)x)^{\frac{x}{1-q}}$  in order to derive the best fit global amplitude  $C$ , temperature  $T$  and entropic index  $q$ . From the best fit parameter  $T$  we derive the average temperature per quark as  $T_0/3$ . The entropic index  $q$  can be translated into effective degrees of freedom  $n$  and into the spectral index  $\gamma$  representing the asymptotic power law behaviour  $\lim_{E \rightarrow \infty} e_q^{-bE} \propto E^\gamma$ .

heliosphere, in particular for charged particles with kinetic energies per nucleon below  $\lesssim 10$  GeV [38]. Thus for our given AMS data with kinetic energies per nucleon in the range of  $0.4 \text{ GeV} \lesssim E \lesssim 1.2 \text{ TeV}$  we would like to quantify the effect of solar wind modulation on our given spectra. Using cosmic ray propagation models allows to infer the unmodulated flux before cosmic rays are entering the heliosphere, that is the local interstellar flux.

This was recently done by [35, 36, 37] who combined the two cosmic ray propagation models HelMod and Galprop and published the calculated flux for all our given atomic nuclei and for the entire energy range covered by AMS. We use their data and interpolate it to match the AMS energy bins definition. We find a maximum deviation of local interstellar flux (LIS) to flux inside heliosphere (AMS) for the lowest energetic particles with  $LIS/AMS \lesssim 4$  for  $E = 0.4 \text{ GeV}$ . The two spectra converge for larger energies quickly and we find  $LIS/AMS \lesssim 1.2$  for  $E = 10 \text{ GeV}$  such that in fact only the lowest energy range of our spectra is significantly affected. Since the propagation model provides the flux without giving any uncertainty, we assign each estimated flux the same relative error as in the AMS data set. This makes the comparison between the flux inside and outside the heliosphere consistent and allows to put appropriate weight on measurements with smaller uncertainties for our least-square optimization.

Analogously to the steps performed for the given AMS data, we apply our generalized statistical mechanics methodology to the LIS data and present the resulting fits and parameters in figure 3. The average temperatures  $T_0/3$  for the different nuclei are about 50 to 80 MeV lower than for the AMS data, namely in the range 129 to 152 MeV. Still, these temperatures are all about the scale of the Hagedorn temperature and in fact coincide with the temperature range 130 to 160 MeV inferred by GSM methods applied to LHC experiments found by [17, 32]. The effective degrees of freedom remain approximately the same. Since the reliability of our methodology ultimately depends on having a large energy range measured for all the different nuclei, the AMS data is the best currently available experimental data set. In contrast, measurements acquired by Voyager outside the heliosphere only cover energies from about 3 MeV to a few hundred MeV [39, 40]. Hence, we apply our analysis to the large range of AMS-measured data and estimate the modulation by the solar wind, rather than using theoretically derived data for unmodulated spectra.

## 6. Conclusion

We provide excellent fits for the measured AMS spectra of primary (He, C, O) and secondary cosmic rays (Li, Be, B) using a simple superstatistical model. The observed  $q$ -exponential spectra are interpreted in terms of temperature fluctuations occurring in the Hagedorn fireball during the production process of cosmic rays in their individual scattering events. We provide evidence that the observed spectra of CR nuclei share universal properties: The spectra collapse if the kinetic energy per nucleon is taken as the relevant variable. Primary and secondary CRs can be uniquely distinguished by

their respective entropic index  $q$ , corresponding to different degrees of freedom associated with the temperature fluctuations. They share the same average temperature parameter, whose order of magnitude coincides with the Hagedorn temperature.

## Acknowledgments

**Acknowledgements** This project has received funding from the European Union's Horizon 2020 research and innovation programme under the Marie Skłodowska–Curie grant agreement No 840825. In addition, we acknowledge support from the DFG Cluster of Excellence 'ORIGINS'.

## Appendix A. Deriving the superstatistical distribution function

We derive the distribution function (1), that is  $P_E = C\rho(E)e_q^{-bE}$ , using the framework of superstatistics by which we can interpret the best fit parameters with a temperature  $T = b^{-1}$  and effective degrees of freedom  $n$ .

Superstatistics [11] is a generalization of Boltzmann statistics in the sense that the distribution function can be derived by integrating the conditional probability distribution  $p_E(E|\beta) = \rho(E)e^{-\beta E}/Z(\beta)$  for all given values of inverse temperature  $\beta$ . The normalization is calculated by summing over all possible energy states, yielding  $Z(\beta) = \int_0^\infty \rho(E)e^{-\beta E}dE$ . In agreement with [13] we apply the ultra-relativistic approximation for the density of states  $\rho(E) \sim E^2$  in order to calculate  $Z(\beta) \sim \beta^{-3}$ . Given the  $\chi^2$ -distributed  $\beta$ , defined by (6), we calculate the generalized canonical distribution as follows:

$$P_E(E) = \int_0^\infty g(\beta)p_E(E|\beta)d\beta \quad (\text{A.1})$$

$$\sim \left(\frac{n}{2\beta_0}\right)^{\frac{n}{2}} \rho(E) \int_0^\infty \beta^{\frac{n}{2}+2} e^{-\beta(E+\frac{n}{2\beta_0})} d\beta \quad (\text{A.2})$$

$$\sim \rho(E) \left(\frac{n}{2\beta_0}\right)^{\frac{n}{2}} \left(E + \frac{n}{2\beta_0}\right)^{-3-\frac{n}{2}}. \quad (\text{A.3})$$

Introducing  $q = 1 + 2/(n + 6)$  (equivalent to  $n/2 = 1/(q - 1) - 3$ ) and  $b = \beta_0/(4 - 3q)$ , allows us to express the result as:

$$P_E(E) \sim \rho(E) \left(E + \frac{n}{2\beta_0}\right)^{-3} \left(\frac{\frac{n}{2\beta_0}}{E + \frac{n}{2\beta_0}}\right)^{\frac{1}{q-1}-3} \quad (\text{A.4})$$

$$\sim \rho(E) \left(\frac{n}{2\beta_0}\right)^{-3} \left(\frac{1}{1 + E\frac{2\beta_0}{n}}\right)^{\frac{1}{q-1}} \quad (\text{A.5})$$

$$\sim \rho(E)e_q^{-bE}. \quad (\text{A.6})$$

Thus we have derived the distribution function (1), which we used for our fits, building on the framework of generalized statistical mechanics and superstatistics.

Note that the above equations are only valid for the particular case  $\rho(E) \sim E^2$  and  $g(\beta)$  being a  $\chi^2$  distribution. More generally, one has

$$P_E(E) \sim \rho(E) \int_0^\infty \frac{g(\beta)}{Z(\beta)} e^{-\beta E} d\beta. \quad (\text{A.7})$$

## Appendix B. Applying theory to observation

We provide a thorough derivation of equation (2), that is  $J_E = v(E)P_E$ , which relates the distribution function from our superstatistical model with the observed differential flux intensity measured by AMS.

The AMS data [1, 2] was published in bins of rigidity  $R = pc/Ze$  with atomic number  $Z$ , electric charge  $e$ , momentum  $p = |\vec{p}|$ ,  $[R] = [\text{V}]$  and the corresponding flux measured in units  $[J(R)] = [\text{m}^{-2}\text{sr}^{-1}\text{s}^{-1}\text{GV}^{-1}]$ . Instead of rigidity we have chosen to investigate the spectrum in respect to kinetic energy per nucleon. To convert the flux dependence from rigidity  $R$  to kinetic energy per nucleon  $E$ , we need to transform the flux  $J_R(R) \rightarrow J_E(E)$  such that  $J_R(R)dR = J_E(E)dE$  is conserved. This is a simple transformation of variables and yields

$$J_E(E) = \frac{A}{Ze} \frac{E + u}{\sqrt{E(E + 2u)}} J_R(R), \quad (\text{B.1})$$

with  $[J_E(E)] = [\text{m}^{-2}\text{sr}^{-1}\text{s}^{-1}\text{GeV}^{-1}]$ . For better visibility of the accuracy of our fits, we multiplied the flux with  $E^{2.7}$ , such that the units for the flux in the presented plots are  $[\text{GeV}^{1.7}\text{m}^{-2}\text{sr}^{-1}\text{s}^{-1}]$ . For the atomic number  $A$  we refer to AMS [1, 2] who inferred the following average abundance of isotopes  $^4\text{He}$ ,  $^{12}\text{C}$ ,  $^{16}\text{O}$ ,  $^{6.5}\text{Li}$ ,  $^8\text{Be}$  and  $^{10.7}\text{Be}$  among the detected nuclei. The measured flux  $J$  represents a differential intensity. Thus it counts the number of particles with energy  $E$  (or rigidity  $R$ ) coming from a unit solid angle that pass through a unit surface per unit of time.

Our superstatistical model builds on a distribution function, denoted as  $P$ , which counts the spatial density of particles within a given momentum/energy range as

$$\frac{dN}{d^3x} \sim P_E(E)dE \sim P_p(E)d^3p. \quad (\text{B.2})$$

Analogously to  $P_E(E) \sim \rho(E)e_q^{-bE}$  in the previous section one can derive that  $P_p(E) \sim e_q^{-bE}$ . Thus the density of states  $\rho(E)$  can be calculated from the conservation condition (B.2). Using  $E = (\sqrt{p^2 + m^2} - m)/A$ , which implies that the energy depends only on the magnitude of the momentum, simplifies  $d^3p = 4\pi p^2 dp$ , and therefore

$$P_E(E) \sim \rho(E)e_q^{-bE} \sim p^2 \frac{dp}{dE} e_q^{-bE}. \quad (\text{B.3})$$

Calculating the derivative and using  $p^2 = A^2 E(E + 2u)$  we find

$$\rho(E) \sim (E + u) \sqrt{E(E + 2u)}. \quad (\text{B.4})$$

Note that we generally neglect constant global factors in our equations because we are focusing on the shape of the spectrum rather than its absolute magnitude. Evidently,  $[p^2 P_p] = [P_E] = [\text{eV}^{-1} \text{m}^{-3}]$  does not have the same dimension as the detected flux,

given as differential intensity  $J$  with  $[J] = [\text{eV}^{-1} \text{m}^{-2} \text{s}^{-1} \text{sr}^{-1}]$ . This reminds us that in order to derive the associated differential intensity from a distribution function we have to account for the rate at which particles go through the detector. That is we multiply with the particle's velocity to obtain the flux  $J_E$ , corresponding to the distribution function  $P_E$ , which yields

$$J_E^{\text{mod}}(E) \sim v(E)P_E(E) \sim v(E)\rho(E)e_q^{-bE}. \quad (\text{B.5})$$

[41] provides a detailed overview about the different ways to count particles including this relation. Evidently, it yields the desired physical dimensions since  $[vP_E] = [\text{eV m}^{-2} \text{s}^{-1}]$ .

In order to express the velocity in terms of  $E$  we use  $p = \gamma mv$  with  $\gamma = \frac{1}{\sqrt{1-v}}$  (in  $c = 1$  convention),  $p = A\sqrt{E(E + 2u)}$  and  $m = Au$  to find

$$v(E) = \frac{\sqrt{E(E + 2u)}}{(E + u)}. \quad (\text{B.6})$$

Plugging everything into (B.5) reveals the relation between q-exponential distribution function and the observed differential intensity

$$J_E^{\text{mod}}(E) = CE(E + 2u)e_q^{-bE} \quad (\text{B.7})$$

which recovers the function we fitted to the data (3).

## References

- [1] M. Aguilar, L. Ali Cavazonza, B. Alpat, G. Ambrosi, L. Arruda, N. Attig, S. Aupetit, P. Azzarello, A. Bachlechner, F. Barao, A. Barrau, L. Barrin, A. Bartoloni, L. Basara, S. Başğmez-du Pree, M. Battarbee, R. Battiston, U. Becker, M. Behlmann, B. Beischer, J. Berdugo, B. Bertucci, K. F. Bindel, V. Bindi, W. de Boer, K. Bollweg, V. Bonnivard, B. Borgia, M. J. Boschini, M. Bourquin, E. F. Bueno, J. Burger, W. J. Burger, F. Cadoux, X. D. Cai, M. Capell, S. Caroff, J. Casaus, G. Castellini, F. Cervelli, M. J. Chae, Y. H. Chang, A. I. Chen, G. M. Chen, H. S. Chen, L. Cheng, H. Y. Chou, E. Choumilov, V. Choutko, C. H. Chung, C. Clark, R. Clavero, G. Coignet, C. Consolandi, A. Contin, C. Corti, W. Creus, M. Crispolti, Z. Cui, K. Dadzie, Y. M. Dai, A. Datta, C. Delgado, S. Della Torre, O. Demakov, M. B. Demirköz, L. Derome, S. Di Falco, F. Dimiccoli, C. Díaz, P. von Doetinchem, F. Dong, F. Donnini, M. Duranti, D. D'Urso, A. Egorov, A. Eline, T. Eronen, J. Feng, E. Fiandrini, P. Fisher, V. Formato, Y. Galaktionov, G. Gallucci, R. J. García-López, C. Gargiulo, H. Gast, I. Gebauer, M. Gervasi, A. Ghelfi, F. Giovacchini, D. M. Gómez-Coral, J. Gong, C. Goy, V. Grabski, D. Grandi, M. Graziani, K. H. Guo, S. Haino, K. C. Han, Z. H. He, M. Heil, J. Hoffman, T. H. Hsieh, H. Huang, Z. C. Huang, C. Huh, M. Incagli, M. Ionica, W. Y. Jang, Yi Jia, H. Jinch, S. C. Kang, K. Kanishev, B. Khiali, G. N. Kim, K. S. Kim, Th. Kirn, C. Konak, O. Kounina, A. Kounine, V. Koutsenko, A. Kulemzin, G. La Vacca, E. Laudi, G. Laurenti, I. Lazzizzera, A. Lebedev, H. T. Lee, S. C. Lee, C. Leluc, H. S. Li, J. Q. Li, Q. Li, T. X. Li, Y. Li, Z. H. Li, Z. Y. Li, S. Lim, C. H. Lin, P. Lipari, T. Lippert, D. Liu, Hu Liu, V. D. Lordello, S. Q. Lu, Y. S. Lu, K. Luebelmeyer, F. Luo, J. Z. Luo, S. S. Lyu, F. Machate, C. Mañá, J. Marín, T. Martin, G. Martínez, N. Masi, D. Maurin, A. Menchaca-Rocha, Q. Meng, V. M. Mikuni, D. C. Mo, P. Mott, T. Nelson, J. Q. Ni, N. Nikonov, F. Nozzoli, A. Oliva, M. Orcinha, F. Palmonari, C. Palomares, M. Panizza, M. Pauluzzi, S. Pensotti, C. Perrina, H. D. Phan, N. Picot-Clemente, F. Pilo, C. Pizzolotto, V. Plyaskin, M. Pohl, V. Poireau, L. Quadrani, X. M. Qi, X. Qin, Z. Y. Qu, T. Rähä, P. G. Rancoita, D. Rapin, J. S. Ricol, S. Rosier-Lees, A. Rozhkov, D. Rozza, R. Sagdeev, S. Schael, S. M. Schmidt, A. Schulz von Dratzig, G. Schwering, E. S. Seo, B. S. Shan,

- J. Y. Shi, T. Siedenburg, D. Son, J. W. Song, M. Tacconi, X. W. Tang, Z. C. Tang, D. Tesaro, Samuel C. C. Ting, S. M. Ting, N. Tomassetti, J. Torsti, C. Türkoğlu, T. Urban, V. Vagelli, E. Valente, E. Valtonen, M. Vázquez Acosta, M. Vecchi, M. Velasco, J. P. Vialle, V. Vitale, S. Vitillo, L. Q. Wang, N. H. Wang, Q. L. Wang, X. Wang, X. Q. Wang, Z. X. Wang, C. C. Wei, Z. L. Weng, K. Whitman, H. Wu, X. Wu, R. Q. Xiong, W. Xu, Q. Yan, J. Yang, M. Yang, Y. Yang, H. Yi, Y. J. Yu, Z. Q. Yu, M. Zannoni, S. Zeissler, C. Zhang, F. Zhang, J. Zhang, J. H. Zhang, S. W. Zhang, Z. Zhang, Z. M. Zheng, H. L. Zhuang, V. Zhukov, A. Zichichi, N. Zimmermann, and P. Zuccon. Observation of the identical rigidity dependence of he, c, and o cosmic rays at high rigidities by the alpha magnetic spectrometer on the international space station. *Physical Review Letter*, 119:251101, Dec 2017.
- [2] M. Aguilar, L. Ali Cavasonza, G. Ambrosi, L. Arruda, N. Attig, S. Aupetit, P. Azzarello, A. Bachlechner, F. Barao, A. Barrau, L. Barrin, A. Bartoloni, L. Basara, S. Başeğmez-du Pree, M. Battarbee, R. Battiston, U. Becker, M. Behlmann, B. Beischer, J. Berdugo, B. Bertucci, K. F. Bindel, V. Bindi, W. de Boer, K. Bollweg, V. Bonnivard, B. Borgia, M. J. Boschini, M. Bourquin, E. F. Bueno, J. Burger, W. J. Burger, F. Cadoux, X. D. Cai, M. Capell, S. Caroff, J. Casaus, G. Castellini, F. Cervelli, M. J. Chae, Y. H. Chang, A. I. Chen, G. M. Chen, H. S. Chen, L. Cheng, H. Y. Chou, E. Choumilov, V. Choutko, C. H. Chung, C. Clark, R. Clavero, G. Coignet, C. Consolandi, A. Contin, C. Corti, W. Creus, M. Crispoltoni, Z. Cui, K. Dadzie, Y. M. Dai, A. Datta, C. Delgado, S. Della Torre, M. B. Demirköz, L. Derome, S. Di Falco, F. Dimiccoli, C. Díaz, P. von Doetinchem, F. Dong, F. Donnini, M. Duranti, D. D’Urso, A. Egorov, A. Eline, T. Eronen, J. Feng, E. Fiandrini, P. Fisher, V. Formato, Y. Galaktionov, G. Gallucci, R. J. García-López, C. Gargiulo, H. Gast, I. Gebauer, M. Gervasi, A. Ghelfi, F. Giovacchini, D. M. Gómez-Coral, J. Gong, C. Goy, V. Grabski, D. Grandi, M. Graziani, K. H. Guo, S. Haino, K. C. Han, Z. H. He, M. Heil, T. H. Hsieh, H. Huang, Z. C. Huang, C. Huh, M. Incagli, M. Ionica, W. Y. Jang, Yi Jia, H. Jinchi, S. C. Kang, K. Kanishev, B. Khiali, G. N. Kim, K. S. Kim, Th. Kirn, C. Konak, O. Kounina, A. Kounine, V. Koutsenko, A. Kulemzin, G. La Vacca, E. Laudi, G. Laurenti, I. Lazzizzera, A. Lebedev, H. T. Lee, S. C. Lee, C. Leluc, H. S. Li, J. Q. Li, Q. Li, T. X. Li, Y. Li, Z. H. Li, Z. Y. Li, S. Lim, C. H. Lin, P. Lipari, T. Lippert, D. Liu, Hu Liu, V. D. Lordello, S. Q. Lu, Y. S. Lu, K. Luebelsmeyer, F. Luo, J. Z. Luo, S. S. Lyu, F. Machate, C. Mañá, J. Marín, T. Martin, G. Martínez, N. Masi, D. Maurin, A. Menchaca-Rocha, Q. Meng, V. M. Mikuni, D. C. Mo, P. Mott, T. Nelson, J. Q. Ni, N. Nikonov, F. Nozzoli, A. Oliva, M. Orcinha, M. Palermo, F. Palmonari, C. Palomares, M. Paniccchia, M. Pauluzzi, S. Pensotti, C. Perrina, H. D. Phan, N. Picot-Clemente, F. Pilo, C. Pizzolotto, V. Plyaskin, M. Pohl, V. Poireau, L. Quadrani, X. M. Qi, X. Qin, Z. Y. Qu, T. Rähkä, P. G. Rancoita, D. Rapin, J. S. Ricol, S. Rosier-Lees, A. Rozhkov, D. Rozza, R. Sagdeev, S. Schael, S. M. Schmidt, A. Schulz von Dratzig, G. Schwering, E. S. Seo, B. S. Shan, J. Y. Shi, T. Siedenburg, D. Son, J. W. Song, M. Tacconi, X. W. Tang, Z. C. Tang, D. Tesaro, Samuel C. C. Ting, S. M. Ting, N. Tomassetti, J. Torsti, C. Türkoğlu, T. Urban, V. Vagelli, E. Valente, E. Valtonen, M. Vázquez Acosta, M. Vecchi, M. Velasco, J. P. Vialle, V. Vitale, L. Q. Wang, N. H. Wang, Q. L. Wang, X. Wang, X. Q. Wang, Z. X. Wang, C. C. Wei, Z. L. Weng, K. Whitman, H. Wu, X. Wu, R. Q. Xiong, W. Xu, Q. Yan, J. Yang, M. Yang, Y. Yang, H. Yi, Y. J. Yu, Z. Q. Yu, M. Zannoni, S. Zeissler, C. Zhang, F. Zhang, J. Zhang, J. H. Zhang, S. W. Zhang, Z. Zhang, Z. M. Zheng, H. L. Zhuang, V. Zhukov, A. Zichichi, N. Zimmermann, and P. Zuccon. Observation of new properties of secondary cosmic rays lithium, beryllium, and boron by the alpha magnetic spectrometer on the international space station. *Physical Review Letter*, 120:021101, Jan 2018.
- [3] Thomas K Gaisser, Ralph Engel, and Elisa Resconi. *Cosmic rays and particle physics*. Cambridge University Press, 2016.
- [4] Vincent Tatischeff and Stefano Gabici. Particle Acceleration by Supernova Shocks and Spallogenic Nucleosynthesis of Light Elements. *Annual Review of Nuclear and Particle Science*, 68(1):377–404, oct 2018.
- [5] Andrew W. Strong, Igor V. Moskalenko, and Vladimir S. Ptuskin. Cosmic-Ray Propagation and

- Interactions in the Galaxy. *Annual Review of Nuclear and Particle Science*, 57(1):285–327, nov 2007.
- [6] Stefano Gabici, Carmelo Evoli, Daniele Gaggero, Paolo Lipari, Philipp Mertsch, Elena Orlando, Andrew Strong, and Andrea Vittino. The origin of Galactic cosmic rays: Challenges to the standard paradigm. *International Journal of Modern Physics D*, 28(15):1930022, nov 2019.
- [7] Grzegorz Wilk and Zbigniew Włodarczyk. Nonextensive thermal sources of cosmic rays. *Central European Journal of Physics*, 8(5):726–736, 2010.
- [8] Constantino Tsallis. Introduction to nonextensive statistical mechanics. *Introduction to Nonextensive Statistical Mechanics*, Springer, 2009.
- [9] Christian Beck. Generalized information and entropy measures in physics. *Contemporary Physics*, 50:495, 2009.
- [10] Petr Jizba and Jan Korbel. Maximum entropy principle in statistical inference: Case for non-shannonian entropies. *Physical Review Letter*, 122:120601, Mar 2019.
- [11] Christian Beck and Ezechiele G D Cohen. Superstatistics. *Physica A: Statistical Mechanics and its Applications*, 322:267–275, 2003.
- [12] Constantino Tsallis, J.C. Anjos, and E.P. Borges. Fluxes of cosmic rays: a delicately balanced stationary state. *Physics Letters A*, 310:372, 2003.
- [13] Christian Beck. Generalized statistical mechanics of cosmic rays. *Physica A Statistical Mechanics and its Applications*, 331(1-2):173–181, 2004.
- [14] G Cigdem Yalcin and Christian Beck. Generalized statistical mechanics of cosmic rays: Application to positron-electron spectral indices. *Scientific Reports*, 8(1):1764, 2018.
- [15] Christian Beck. Superstatistics in high-energy physics. *The European Physical Journal A*, 40(3):267, 2009.
- [16] L. Marques, E. Andrade-II, and A. Deppman. Nonextensivity of hadronic systems. *Physical Review D*, 87:114022, Jun 2013.
- [17] Cheuk-Yin Wong, Grzegorz Wilk, Leonardo J. L. Cirto, and Constantino Tsallis. From qcd-based hard-scattering to nonextensive statistical mechanical descriptions of transverse momentum spectra in high-energy  $pp$  and  $p\bar{p}$  collisions. *Physical Review D*, 91:114027, Jun 2015.
- [18] Christian Beck. Statistics of three-dimensional lagrangian turbulence. *Physical Review Letter*, 98:064502, Feb 2007.
- [19] Karen E Daniels, Christian Beck, and Eberhard Bodenschatz. Defect turbulence and generalized statistical mechanics. *Physica D: Nonlinear Phenomena*, 193(1-4):208–217, 2004.
- [20] Salvo Rizzo and Andrea Rapisarda. Environmental atmospheric turbulence at florence airport. In *AIP Conference Proceedings*, volume 742, pages 176–181. AIP, 2004.
- [21] Juliane Weber, Mark Reyers, Christian Beck, Marc Timme, Joaquim G Pinto, Dirk Witthaut, and Benjamin Schäfer. Wind power persistence is characterized by superstatistics. *Scientific Reports*, 9:19971, 2019.
- [22] Benjamin Schäfer, Christian Beck, Kazuyuki Aihara, Dirk Witthaut, and Marc Timme. Non-gaussian power grid frequency fluctuations characterized by lévy-stable laws and superstatistics. *Nature Energy*, 3(2):119, 2018.
- [23] L. R. Gorjão, M. Anvari, H. Kantz, C. Beck, D. Witthaut, M. Timme, and B. Schäfer. Data-driven model of the power-grid frequency dynamics. *IEEE Access*, 8:43082–43097, 2020.
- [24] Griffin Williams, Benjamin Schäfer, and Christian Beck. Superstatistical approach to air pollution statistics. *Physical Review Research*, 2:013019, 2020.
- [25] Christian Beck. Dynamical foundations of nonextensive statistical mechanics. *Physical Review Letter*, 87:180601, Oct 2001.
- [26] E Gravanis, E Akylas, and G Livadiotis. Physical meaning of temperature in superstatistics. *EPL (Europhysics Letter)*, 130(3):30005, 2020.
- [27] Rolf Hagedorn. Statistical thermodynamics of strong interactions at high energies. *Nuovo Cimento, Suppl.*, 3(CERN-TH-520):147–186, 1965.
- [28] Johann Rafelski and Torleif Ericson. The Tale of the Hagedorn Temperature BT - Melting Hadrons,



- Boiling Quarks - From Hagedorn Temperature to Ultra-Relativistic Heavy-Ion Collisions at CERN: With a Tribute to Rolf Hagedorn. pages 41–48. Springer International Publishing, Cham, 2016.
- [29] Wojciech Broniowski, Wojciech Florkowski, and Leonid Ya. Glozman. Update of the Hagedorn mass spectrum. *\prd*, 70(11):117503, dec 2004.
- [30] Christian Beck. Non-extensive statistical mechanics and particle spectra in elementary interactions. *Physica A: Statistical Mechanics and its Applications*, 286(1):164–180, oct 2000.
- [31] J M Lattimer. Introduction to neutron stars. *AIP Conference Proceedings*, 1645(1):61–78, 2015.
- [32] Grzegorz Wilk and Zbigniew Włodarczyk. Oscillations in Multiparticle Production Processes. *Entropy*, 19(12):670, dec 2017.
- [33] A Deppman. Thermodynamics with fractal structure, Tsallis statistics, and hadrons. *Physical Review D*, 93(5):54001, mar 2016.
- [34] I Bediaga, E. M. F. Curado, and J. M. de Miranda. A nonextensive thermodynamical equilibrium approach in  $e+e\rightarrow$  hadrons. *Physica A: Statistical Mechanics and its Applications*, 286(1):156–163, oct 2000.
- [35] M. J. Boschini, S. Della Torre, M. Gervasi, D. Grandi, G. Jóhannesson, M. Kachelriess, G. La Vacca, N. Masi, I. V. Moskalenko, E. Orlando, S. S. Ostapchenko, S. Pensotti, T. A. Porter, L. Quadrani, P. G. Rancoita, D. Rozza, and M. Tacconi. Solution of Heliospheric Propagation: Unveiling the Local Interstellar Spectra of Cosmic-ray Species. *Astrophysical Journal*, 840(2):115, 2017.
- [36] M J Boschini, S Della Torre, M Gervasi, D Grandi, G Jóhannesson, G La Vacca, N Masi, I V Moskalenko, S Pensotti, T A Porter, L Quadrani, P G Rancoita, D Rozza, and M Tacconi. Deciphering the Local Interstellar Spectra of Primary Cosmic-Ray Species with {HelMod}. *Astrophysical Journal*, 858(1):61, may 2018.
- [37] M. J. Boschini, S. Della Torre, M. Gervasi, D. Grandi, G. Jóhannesson, G. La Vacca, N. Masi, I. V. Moskalenko, S. Pensotti, T. A. Porter, L. Quadrani, P. G. Rancoita, D. Rozza, and M. Tacconi. Deciphering the Local Interstellar Spectra of Secondary Nuclei with the Galprop/Helmod Framework and a Hint for Primary Lithium in Cosmic Rays. *Astrophysical Journal*, 889(2):167, 2020.
- [38] Harm Moraal. Cosmic rays in the heliosphere: Observations. *Astroparticle Physics*, 53:175–185, jan 2014.
- [39] A. C. Cummings, E. C. Stone, B. C. Heikkila, N Lal, W. R. Webber, G Jóhannesson, I. V. Moskalenko, E Orlando, and T. A. Porter. Galactic Cosmic Rays in the Local Interstellar Medium: Voyager 1 Observations and Model Results. *Astrophys. J.*, 831(1):18, nov 2016.
- [40] Edward C. Stone, Alan C. Cummings, Bryant C. Heikkila, and Nand Lal. Cosmic ray measurements from Voyager 2 as it crossed into interstellar space. *Nat. Astron.*, 3(11):1013–1018, nov 2019.
- [41] H. Moraal. Cosmic-ray modulation equations. *Space Science Reviews*, 176(1-4):299–319, jun 2013.